# Recent advances in understanding structure–function relationships in the type II topoisomerase mechanism

**A.J. Schoeffler and J.M. Berger[1]**
Department of Molecular and Cell Biology, 237 Hildebrand Hall #3206, University of California, Berkeley, CA 94720-3206, U.S.A.

## Abstract

**DNA topos (topoisomerases) are complex, multisubunit enzymes that remodel DNA topology. Members of the type II topo family function by passing one segment of duplex DNA through a transient break in another, a process that consumes two molecules of ATP and requires the co-ordinated action of multiple domains. Recent structural data on type II topo ATPase regions, which activate and enforce the directionality of DNA strand passage, have highlighted how ATP physically controls the catalytic cycle of the enzyme. Structural and biochemical studies of specialized DNA-binding domains in two paralogous bacterial type IIA topos (DNA gyrase and topo IV) show how these enzymes selectively negatively supercoil or decatenate DNA. Taken together, these findings expand our understanding of how disparate functional elements work together to co-ordinate the type II topo mechanism.**

## Introduction

The double helical structure of DNA, due to the intertwining of its complementary strands, is prone to topological problems. For example, processive unwinding of the double helix promotes the under- and over-winding of adjacent duplex regions, generating a superhelical strain that, if left unresolved, can impair replication and transcription [1]. As the chromosome is duplicated and packaged, DNA tangles and knots, structures that can result in double-stranded DNA breaks and chromosome partitioning defects, also can arise [2,3].

To resolve these DNA superstructures, cells rely on essential enzymes known as DNA topos (topoisomerases). Topos are divided into two families, type I and II, on the basis of their different architectures and mechanisms [4,5]. Type II topos, the focus of this review, remodel DNA topology by passing one double-stranded DNA segment through a transient, enzyme-mediated break in another, a process that requires two molecules of ATP and the co-ordinated activity of several constituent domains [4,5]. This complex interplay of functions has generated significant interest in understanding topos as molecular machines. In addition, because corruption of their catalytic cycle can lead to cytotoxic double-stranded DNA breaks, topos are important targets of antibacterial and anticancer agents. Understanding the topo mechanism is therefore of great medical importance as well.

**Key words:** C-terminal domain (CTD), DNA topology, GHKL ATPase, gyrase, $\beta$-pinwheel, topoisomerase.

**Abbreviations used:** CAP, catabolite gene activator protein; CTD and NTD, C- and N-terminal domains respectively; G- and T-segments, gate and transfer segments respectively; topo, topoisomerase.

[1]To whom correspondence should be addressed (email jmberger@berkeley.edu).

## Type IIA topo structure and general mechanism

Type II topos are divided into A and B subfamilies on the basis of sequence and structure, but all of these proteins possess a core set of conserved ATPase and DNA-binding domains [4,5]. Within a holoenzyme, pairs of like domains form dimer interfaces, termed gates, that control the passage of DNA through the enzyme (Figure 1A). The type IIA topo reaction (Figure 1B) begins when a double-stranded DNA segment, termed the G-segment (gate segment), binds to two catalytic elements [the toprim and 5Y-CAP (catabolite gene activator protein) domains] that form the DNA gate [4,5]. A second segment of double-stranded DNA [the T-segment (transfer segment)] is then captured by the ATP-induced dimerization of the ATPase domains (the ATP gate), which are composed of two functional modules termed the GHKL (for gyrase, heat-shock protein 90, histidine kinase and MukL) and transducer domains [6–8]. Capture and dimerization lead to G-segment cleavage and opening, after which the T-segment (transfer segment) is passed through the G-segment gap [9]. Following this event, the G-segment is religated, and a third dimer interface (the C-gate) is thought to open to permit escape of the T-segment [10–12]. ADP release, followed by opening of the ATP gate, then resets the enzyme for another round of catalysis. In the cell, this ATP-dependent duplex strand passage mechanism enables type II topos to catalyse supercoil relaxation and introduction, decatenation and catenation, or knotting and unknotting, thereby actively remodelling chromosome superstructures [4,5].

©2005 Biochemical Society

**Figure 1 | Proposed general quaternary structure and catalytic mechanism of type IIA topos**

(**A**) Model for the general arrangement of type IIA topo elements. ATPase domains are shown in yellow (the GHKL subdomain) and orange (the transducer subdomain), with the N-terminal straps represented by black lines. The DNA gate is formed by two 5Y-CAP domains (green); a pair of toprim folds (red) assists with the catalysis of DNA cleavage. The tower domains are coloured light blue, the C-gate dark blue and the CTD purple. The 2-fold symmetry axis of the holoenzyme is indicated by a dashed line; eukaryotic type II topo is expressed as a homodimer whereas prokaryotic enzymes are heterotetramers. Bacterial GyrB/ParE subunits encompass the ATPase, transducer and toprim folds, while the GyrA and ParC subunits comprise the other elements. (**B**) Schematic representation of the type IIA topo catalytic cycle. Domains are coloured as in (**A**). The G-segment (pale green) first binds to the DNA gate (step 1). A T-segment (teal) is captured by dimerization of the ATPase domains upon ATP (black star) binding (step 2). ATP hydrolysis followed by $P_i$ release triggers DNA gate opening and T-segment passage (step 3). C-gate opening allows escape of the T-segment (step 4), while religation of the G-segment and release of hydrolysis products lead to opening of the ATP gate, thus resetting the enzyme for another round of catalysis (step 1).

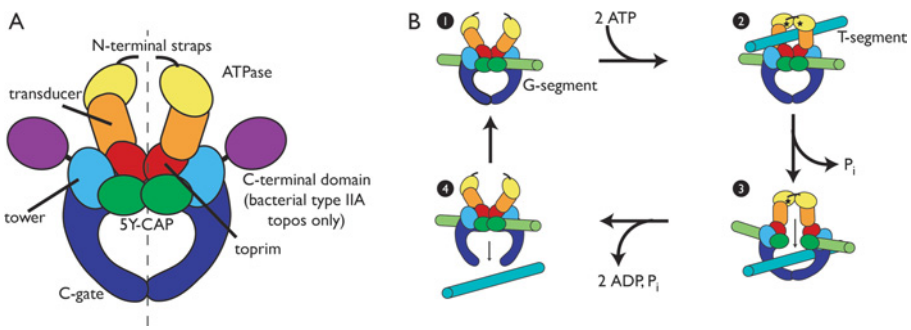


## ATPase domains dimerize upon nucleotide binding and sequester nucleotide from solvent

Much progress has been made towards understanding the physical basis by which ATP binding generates the large-scale conformational changes that initiate the duplex passage reaction. Numerous structural studies have shown that ATP binding within a subunit causes a reordering of structural elements that favours dimerization of the ATPase domains [6,13,14]. The ATPase domain dimer is stabilized by substantial interprotomer contacts as well as by an N-terminal motif called the 'strap', which comprises 15 residues that extend from one monomer to dock into the ATP-binding site of the other [6,13,14]. Once formed, this quaternary arrangement sequesters nucleotide deep within a solvent-shielded binding site [6,13,14]. The inaccessibility of the bound nucleotide forces the ATP gate to remain closed until conformational changes enable nucleotide release, thus preventing T-segment escape.

## $P_i$ release provides a mechanism of communication between ATP turnover and strand passage

In addition to initiating the strand passage reaction, the ATPase domains of type II topos also regulate the rate of DNA cleavage and T-segment transport. There is evidence of significant communication between these functions. ATP hydrolysis is not required for single enzyme turnover, but it significantly (20–30-fold) accelerates the reaction [9,15–17]. Kinetic studies have suggested that $P_i$ release is involved in this communication, revealing that the two ATPs bound by type II topos are hydrolysed asynchronously and that strand passage is probably accompanied by the release of $P_i$ from the first hydrolysis event [15,18,19]. The structural mechanisms by which this crosstalk occurs, however, have remained unclear.

## $P_i$ release is linked to conformational changes within the ATPase domains

A structural study of the ATPase domains of topo VI (topo VI B′), carried out in the presence of different nucleotides and nucleotide analogues, has begun to address the question of how ATP turnover and DNA strand passage are coupled [20,21]. This work, which completely defines the ATP turnover cycle for a type II topo, reveals that the ATPase domains can adopt two conformations that are distinct from quaternary changes that occur during the monomer–dimer transition [21]. One conformation, termed the restrained state, forms upon ATP binding and appears to persist throughout hydrolysis and product formation [21]. The other, the relaxed state, is observed in nucleotide-free protein [21]. In the restrained state, the $\gamma$-phosphate is co-ordinated by an $Mg^{2+}$ ion, several main-chain nitrogens within a region called the ATP lid, and a conserved lysine residue (the 'switch lysine') that protrudes from the transducer domain [21]. This conformation is sustained when the $\gamma$-phosphate is replaced with $AlF_4^-$ (a transition-state analogue) or $P_i$ (mimicking the product-bound state) [21]. In contrast, in the relaxed state, the ATP lid adopts an alternative configuration and the

©2005 Biochemical Society

**Figure 2 | Conformational changes in the topo VI ATPase domain**

(**A**) Upper panel: nucleotide-binding region of one monomer of the dimeric ATPase domain of topo VI bound to ADP · $P_i$. The GHKL domain is shown in gold and the transducer domain in orange. ADP and $P_i$ are represented by a stick models, bound $Mg^{2+}$ by a green sphere and the switch lysine by a stick model. Lower panel: nucleotide-binding region of ADP-bound topo VI ATPase domain monomer. Orientation is the same as in the upper panel. Note that the switch lysine has flipped out of the active site. The ATP lid also is reorganized. (**B**) Monomeric, ADP-bound, relaxed form of the topo VI ATPase domain superposed on one subunit of the dimerized ADP • $P_i$-restrained form. The C$\alpha$ backbone of the monomer is shown in yellow; that of the dimer is shown in grey and blue. The GHKL domains of the two structures were aligned using PyMOL (DeLano Scientific, San Francisco, CA, U.S.A.). The switch lysine (shown as a stick model) is shown in its two conformations (red for restrained and green for relaxed). The transition from the restrained to relaxed state results in the C-terminal helix of the transducer rotating outward by 11° (arrow). (**C**) Proposed model for the interplay of $P_i$ release and T-segment passage. The GHKL and transducer domains, together with the G- and T-segments, are coloured as in Figure 1; ATP is represented by a black star and ADP by a white star. Upon T-segment capture by the dimerization of the ATPase domains, it may exert strain on the closed ATP gate (wavy lines, leftmost panel). This strain may help trigger a restrained-to-relaxed transition (rotation of the transducer and release of $P_i$) in one of the ATPase domains, leading to opening of the DNA gate and T-segment passage (middle panel). After DNA gate closure and G-segment religation, the second ATP is hydrolysed and all hydrolysis products are released from both ATPase domains, opening the ATP gate in preparation for the next round of strand passage (rightmost panel).

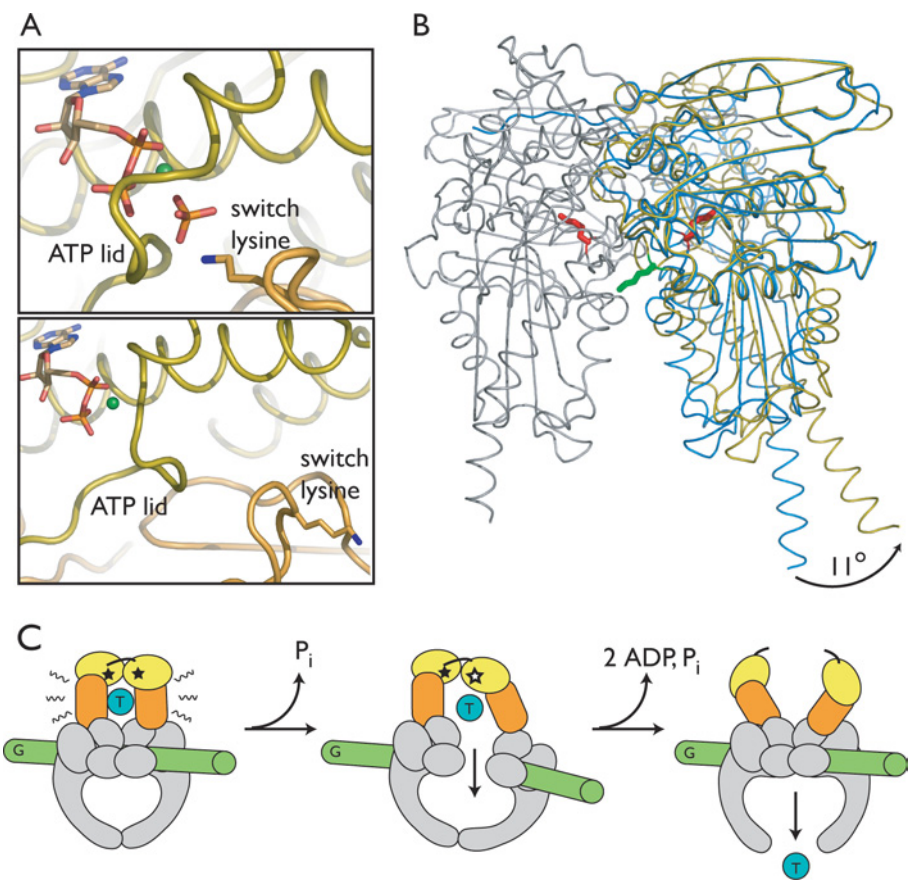


switch lysine of the transducer domain undergoes a dramatic outward flip to become solvent-exposed (Figures 2A and 2B) [20,21]. This motion propagates through the transducer domain to rotate the C-terminal-most helix outward by approx. 11° (Figure 2B) [21]. Given the observation that the nucleotide-binding site is completely buried, it is likely that the restrained-to-relaxed transition is necessary for $P_i$ release [21]. Consistent with this idea, the same structural study shows that ADP binding can support both states [20,21].

These observations provide an architectural framework for understanding the roles of ATP hydrolysis and $P_i$ release in the type II topo mechanism. Taken together, the ensemble of ATPase domain structures suggests that the initial $P_i$ release event thought to accompany T-segment transport

©2005 Biochemical Society

may be dependent on rotation of the transducer domain and movement of its switch lysine out of the active site. Because the transducer region is physically linked to the DNA gate, this movement may be coupled simultaneously with opening of the G-segment. Although the driving force behind these conformational changes remains unknown, it may be provided by the T-segment itself. T-segment binding appears to be necessary for efficient G-segment cleavage, and creation of a point mutation that widens the ATP gate cavity (from 13 to ~20 Å; 1 Å = 0.1 nm) decouples ATP turnover and duplex passage [22,23]. These results suggest that T-segment binding to the ATP gate cavity may produce a strain that would encourage the restrained-to-relaxed transition and thus DNA gate opening. Such a scheme would account for the ability of non-hydrolysable ATP analogues to support a single round of strand passage, since T-segment capture would be sufficient to drive G-segment separation [9,15–17]. It would also explain why ATP hydrolysis accelerates the strand passage reaction: the covalent $\beta$–$\gamma$ phosphate bond would act as a cleavable interdomain cross-linker that, upon breakage, would free the GHKL and transducer domains to reorientate for T-segment passage [15].

## Bacterial type IIA topos have specialized functions

Although ATP binding and turnover is the central controller of the type II topo reaction, some members of this enzyme superfamily have auxiliary domains that exert additional levels of control, biasing activity towards execution of a subset of topological transformations. Bacteria express two type IIA topo paralogues (DNA gyrase and topo IV) with distinct and unique functions [4,5]. DNA gyrase introduces negative supercoils into DNA, maintaining bacterial chromosomes in an underwound state to promote compaction and unwinding [24,25]. In contrast, topo IV is an efficient decatenase, separating tangled daughter chromosomes following replication [2,26,27]. Both enzymes are heterotetramers, with the ATPase and toprim domains combined within the GyrB (for gyrase) and ParE (for topo IV) subunits, and the 5Y-CAP and C-gate regions combined within GyrA and ParC [4,5]. The GyrA and ParC subunits both include a globular domain at their C-terminus, termed the CTD (C-terminal domain), whose presence is unique to bacterial type IIA topos. The physical basis by which these homologous domains cooperate to support the different biochemical activities of gyrase and topo IV has recently become a topic of great interest.

## The CTDs of gyrase and topo IV adopt $\beta$-pinwheel folds

Within the last year, efforts from several groups have provided structural information on bacterial type IIA topo CTDs. The structures available to date include the CTDs of *Escherichia coli* GyrA and ParC, *Bacillus stearothermophilus* ParC and *Borrelia burgdorferi* GyrA (Figure 3A) [28–31]. These studies reveal that the ParC and GyrA CTDs adopt a unique fold, termed a $\beta$-pinwheel [30]. The $\beta$-pinwheel fold is superficially similar to a $\beta$-propeller in that it consists of radially arranged repeating units (blades) made up of four $\beta$-strands each; however, unlike the $\beta$-propeller, which is composed of blades built on a sequential $\beta$-hairpin motif, the blades of the $\beta$-pinwheel are derived from a Greek-key topology [30]. In all observed instances to date, the outer rim of the $\beta$-pinwheel fold is positively charged, and is thought to be a DNA-binding and -bending surface [28–31].

Surprisingly, there is significant structural diversity among the four homologous CTDs (Figure 3A). The *Bo. burgdorferi* GyrA CTD adopts a closed $\beta$-pinwheel fold, while the equivalent domains from *E. coli* GyrA and ParC and *Ba. stearothermophilus* ParC are broken open [28–31]. The folds of the *E. coli* ParC CTD and the *Bo. burgdorferi* GyrA CTD are both relatively planar, while the *Ba. stearothermophilus* ParC CTD and the *E. coli* GyrA CTD adopt similar spiral conformations [28–31]. Out of the four, only the *E. coli* ParC CTD has five blades instead of six; however, secondary-structure predictions indicate that orthologous ParC CTDs may have as few as three or as many as eight blades, or may lack a CTD entirely [29]. In contrast, nearly all GyrA CTDs appear to possess six blades plus a conserved signature sequence element called the GyrA box [29]. Given the biochemical data currently available, it appears that gyrases require a six-bladed CTD, while topo IV's requirements are less stringent.

## Bacterial type IIA topo CTDs control substrate selectivity and topological transformation activity

Mounting evidence indicates that the CTDs of ParC and GyrA have a profound effect on holoenzyme activity. Truncation of the CTD from *E. coli* gyrase abrogates its ability to negatively supercoil DNA [32,33]. Biochemical studies of GyrA CTDs in isolation show that they can bind and induce positive writhe in DNA, stabilizing a DNA bend of approx. 180° [30,31,33]. Recent work reveals that the ParC CTD, like the GyrA CTD, is responsible for controlling the specific topological transformation activity of the holoenzyme. Topo IV is a highly active decatenase and is 10–20-fold more efficient at relaxing positive supercoils than negative supercoils [27,29,34]. Truncation of the ParC CTD abolishes this preference and reduces enzyme activity to similar basal levels on all substrates [29]. Like the GyrA CTD, the ParC domain in isolation can bind and bend DNA, but with much less efficacy [30]. In addition, the topo IV holoenzyme introduces negligible writhe in DNA, so it is likely that the ParC CTD cannot induce writhe in DNA as the GyrA CTD can [35].

How can one element impart such disparate functional properties to bacterial type IIA topos? Clues have come from structural studies of the full-length GyrA and ParC subunits. For gyrase, the position of the CTD in the holoenzyme complex has been inferred from low-resolution structural data. Electron micrographs and small angle X-ray scattering studies suggest that the CTDs can dock either near the

©2005 Biochemical Society

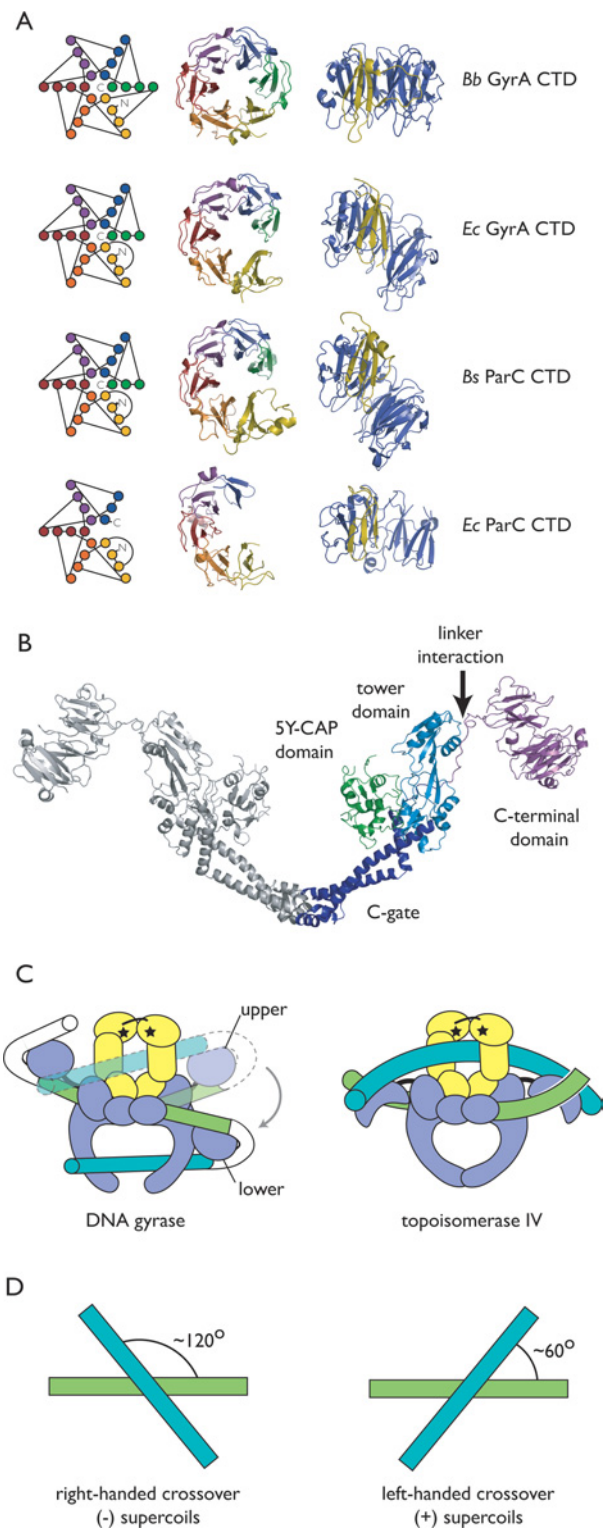


**Figure 3 | CTD structure and orientation in bacterial type IIA topos**

(**A**) CTD structure. From top to bottom, the *Bo. burgdorferi* GyrA CTD, the *E. coli* GyrA CTD, the *Ba. stearothermophilus* ParC CTD and the *E. coli* ParC CTD are shown. All CTDs adopt $\beta$-pinwheel folds, as depicted in topology diagrams on the left. The blades interlock, with the outermost strand of each blade packing against the second outermost strand of the adjacent blade. The crystal structure of each domain is shown in the middle, in the same general orientation as the topology diagrams. Note that only the *Bo. burgdorferi* GyrA CTD adopts a closed $\beta$-pinwheel fold, while the rest are broken open. On the right, each CTD is viewed edge-on, rotated 90° into the plane of the page. Blade 1 (in gold) of each CTD was aligned to corresponding residues of the *Bo. burgdorferi* CTD to highlight the spiral conformation of the *E. coli* GyrA CTD and the *Ba. stearothermophilus* ParC CTD. Structural alignments were performed using PyMOL (DeLano Scientific). (**B**) Structure of *E. coli* ParC. The protein crystallized as a dimer, with the primary dimer interface at the C-gate (dark blue). The CTD (purple) is docked at the top of the tower domain (light blue) through an extended linker. The 5Y-CAP domain is shown in green. One monomer is shown in grey for clarity. (**C**) Proposed catalytic mechanisms of DNA gyrase (left) and topo IV (right). GyrB and ParE are coloured yellow and GyrA and ParC violet. T- and G-segments are coloured teal and pale green respectively. DNA gyrase (left) uses its CTDs to wrap the G-segment as it exits the DNA gate and then reintroduces the DNA segment to the enzyme as a T-segment *in cis*. The CTD may alternate between upper and lower positions, moving with the T-segment as it passes through the DNA gate. Topo IV's (right) CTDs do not efficiently bend DNA or adopt multiple positions in the holoenzyme. The CTDs are anchored in a position where they may preferentially bind T-segments of a left-handed crossover geometry relative to the bound G-segment. The curved DNA-binding surface presented by the CTDs may facilitate recognition of the 'hooked juxtapositions' that are prevalent in catenated DNA. (**D**) Geometry of DNA crossovers. Right-handed crossovers (left) are prevalent in negatively supercoiled DNA, while left-handed crossovers (right) are prevalent in positively supercoiled DNA.

tower domain of the GyrA subunit or near the C-gate (Figure 1) [36,37]. These observations are in agreement with the prediction that the CTD and NTD (N-terminal domain) of GyrA are connected by a flexible linker. In contrast, a recent structure of the *E. coli* ParC subunit shows that the CTD is anchored into the tower domain by hydrophobic interactions [29]. In both gyrase and topo IV, the upper placement of the CTD (near the tower domain) appears to position the domain to facilitate interactions with an incoming T-segment.

From these observations, several models have emerged to account for the distinct activities of gyrase and topo IV (Figure 3C). Because the GyrA CTD can strongly bind and bend DNA, this domain appears to be capable of wraping a G-segment extending out from the DNA gate back towards the gyrase holoenzyme, providing a T-segment *in cis* [30,38]. This wrap enforces a positive-handed crossover geometry between the G- and T-segments, which leads to the introduction of negative supercoils upon strand passage [30,38]. The flexibility of the GyrA NTD/CTD linker may allow the CTD to oscillate between two positions over the course of the catalytic cycle, perhaps as a means of shuttling the T-segment through the enzyme. In contrast, the CTD of topo IV, by virtue of its weaker DNA-binding and -bending activity, is likely to interact more favourably with T-segments provided to the enzyme *in trans*. The docked configuration of the ParC CTD may allow it to favour binding to T-segments that form a left-handed crossover with the G-segment,

©2005 Biochemical Society

a geometry that is prevalent in positively supercoiled DNA [29,39] (Figure 3D). Unrestrained T-segments that come from a distal region of the DNA or a separate DNA molecule also would be favoured [29]. It is additionally possible that the curved DNA-binding surface presented by the topo IV CTD preferentially recognizes specialized T- and G-segment arrangements known as hooked juxtapositions, which characterize topologically linked DNA molecules [40].

## Future directions

We are beginning to grasp certain aspects of how the complex mechanisms of type II topos emerge from the articulated and co-ordinated action of multiple conserved domains. Recent work on the ATPase domains of topo VI has highlighted how the energy of ATP hydrolysis may be directed to regulate concerted conformational changes. New structural and biochemical studies of gyrase and topo IV have revealed how an auxiliary structural element can lead to significant mechanistic and physiological consequences. Nevertheless, many questions still remain. For example, our understanding of the topo mechanism still requires the determination of high-resolution structures of DNA bound to type II topos. Such information will help us to understand many aspects of function, such as how the GyrA CTD generates writhe and how the DNA gate interacts with DNA. Study of these enzymes has a long history, but their complexity still offers rich avenues of inquiry for the future.

## Note added in proof (received 8 September 2005)

In a recent crystallographic study of the human topo II ATPase domain, Verdine and colleagues observed structural changes similar to those reported for topo IV, including a 10° rotation of the transducer domain and a reorientation of the switch lysine between nucleotide binding and release. They also observed a new conformation of the C-terminus of the transducer domain when the protein is bound to ADP [41].

A.J.S. acknowledges support from an NSF (National Science Foundation) Graduate Research Fellowship. This work was supported by the National Cancer Institute (CA77373).

## References

1 Wu, H.Y., Shyy, S., Wang, J.C. and Liu, L.F. (1988) Cell (Cambridge, Mass.) **53**, 433–440
2 Kato, J., Nishimura, Y., Imamura, R., Niki, H., Hiraga, S. and Suzuki, H. (1990) Cell (Cambridge, Mass.) **63**, 393–404
3 Hiraga, S. (1990) Res. Microbiol. **141**, 50–56
4 Corbett, K.D. and Berger, J.M. (2004) Annu. Rev. Biophys. Biomol. Struct. **33**, 95–118
5 Champoux, J.J. (2001) Annu. Rev. Biochem. **70**, 369–413
6 Wigley, D.B., Davies, G.J., Dodson, E.J., Maxwell, A. and Dodson, G. (1991) Nature (London) **351**, 624–629
7 Ali, J.A., Orphanides, G. and Maxwell, A. (1995) Biochemistry **34**, 9801–9808
8 Ali, J.A., Jackson, A.P., Howells, A.J. and Maxwell, A. (1993) Biochemistry **32**, 2717–2724
9 Sugino, A., Higgins, N.P. and Cozzarelli, N.R. (1980) Nucleic Acids Res. **8**, 3865–3874
10 Roca, J., Berger, J.M., Harrison, S.C. and Wang, J.C. (1996) Proc. Natl. Acad. Sci. U.S.A. **93**, 4057–4062
11 Roca, J. and Wang, J.C. (1994) Cell (Cambridge, Mass.) **77**, 609–616
12 Morais Cabral, J.H., Jackson, A.P., Smith, C.V., Shikotra, N., Maxwell, A. and Liddington, R.C. (1997) Nature (London) **388**, 903–906
13 Classen, S., Olland, S. and Berger, J.M. (2003) Proc. Natl. Acad. Sci. U.S.A. **100**, 10629–10634
14 Bellon, S., Parsons, J.D., Wei, Y.Y., Hayakawa, K., Swenson, L.L., Charifson, P.S., Lippke, J.A., Aldape, R. and Gross, C.H. (2004) Antimicrob. Agents Chemother. **48**, 1856–1864
15 Baird, C.L., Harkins, T.T., Morris, S.K. and Lindsley, J.E. (1999) Proc. Natl. Acad. Sci. U.S.A. **96**, 13685–13690
16 Williams, N.L., Howells, A.J. and Maxwell, A. (2001) J. Mol. Biol. **306**, 969–984
17 Osheroff, N., Shelton, E.R. and Brutlag, D.L. (1983) J. Biol. Chem. **258**, 9536–9543
18 Harkins, T.T., Lewis, T.J. and Lindsley, J.E. (1998) Biochemistry **37**, 7299–7312
19 Baird, C.L., Gordon, M.S., Andrenyak, D.M., Marecek, J.F. and Lindsley, J.E. (2001) J. Biol. Chem. **276**, 27893–27898
20 Corbett, K.D. and Berger, J.M. (2003) EMBO J. **22**, 151–163
21 Corbett, K.D. and Berger, J.M. (2005) Structure **13**, 873–882
22 Tingey, A.P. and Maxwell, A. (1996) Nucleic Acids Res. **24**, 4868–4873
23 Corbett, A.H., Zechiedrich, E.L. and Osheroff, N. (1992) J. Biol. Chem. **267**, 683–686
24 Vologodskii, A.V. and Cozzarelli, N.R. (1994) Annu. Rev. Biophys. Biomol. Struct. **23**, 609–643
25 Holmes, V.F. and Cozzarelli, N.R. (2000) Proc. Natl. Acad. Sci. U.S.A. **97**, 1322–1324
26 Deibler, R.W., Rahmati, S. and Zechiedrich, E.L. (2001) Genes Dev. **15**, 748–761
27 Zechiedrich, E.L., Khodursky, A.B. and Cozzarelli, N.R. (1997) Genes Dev. **11**, 2580–2592
28 Hsieh, T.J., Farh, L., Huang, W.M. and Chan, N.L. (2004) J. Biol. Chem. **279**, 55587–55593
29 Corbett, K.D., Schoeffler, A.J., Thomsen, N.D. and Berger, J.M. (2005) J. Mol. Biol. **351**, 545–561
30 Corbett, K.D., Shultzaberger, R.K. and Berger, J.M. (2004) Proc. Natl. Acad. Sci. U.S.A. **101**, 7293–7298
31 Ruthenburg, A.J., Graybosch, D.M., Huetsch, J.C. and Verdine, G.L. (2005) J. Biol. Chem. **280**, 26177–26184
32 Kampranis, S.C. and Maxwell, A. (1996) Proc. Natl. Acad. Sci. U.S.A. **93**, 14416–14421
33 Reece, R.J. and Maxwell, A. (1991) Nucleic Acids Res. **19**, 1399–1405
34 Crisona, N.J., Strick, T.R., Bensimon, D., Croquette, V. and Cozzarelli, N.R. (2000) Genes Dev. **14**, 2881–2892
35 Peng, H. and Marians, K.J. (1995) J. Biol. Chem. **270**, 25286–25290
36 Kirchhausen, T., Wang, J.C. and Harrison, S.C. (1985) Cell (Cambridge, Mass.) **41**, 933–943
37 Costenaro, L., Grossmann, J.G., Ebel, C. and Maxwell, A. (2005) Structure **13**, 287–296
38 Kampranis, S.C., Bates, A.D. and Maxwell, A. (1999) Proc. Natl. Acad. Sci. U.S.A. **96**, 8414–8419
39 Stone, M.D., Bryant, Z., Crisona, N.J., Smith, S.B., Vologodskii, A., Bustamante, C. and Cozzarelli, N.R. (2003) Proc. Natl. Acad. Sci. U.S.A. **100**, 8654–8659
40 Buck, G.R. and Zechiedrich, E.L. (2004) J. Mol. Biol. **340**, 933–939
41 Wei, H., Ruthenburg, A.J., Bechis, S.K. and Verdine, G.L. (2005) J. Biol. Chem., doi:10.1074/jbc.M506520200

Received 17 June 2005

©2005 Biochemical Society